Atmospheric Environment 172 (2018) 83–92

Contents lists available at ScienceDirect

Atmospheric Environment

journal homepage: www.elsevier.com/locate/atmosenv

Seasonal impact of regional outdoor biomass burning on air pollution in three Indian cities: Delhi, Bengaluru, and Pune

Tianjia Liu[a,*], Miriam E. Marlier[b], Ruth S. DeFries[b], Daniel M. Westervelt[c,d], Karen R. Xia[e], Arlene M. Fiore[a,c], Loretta J. Mickley[f], Daniel H. Cusworth[g], George Milly[c]

[a] Department of Earth and Environmental Sciences, Columbia University, New York, 10027, USA
[b] Department of Ecology, Evolution, and Environmental Biology, Columbia University, New York, 10027, USA
[c] Lamont-Doherty Earth Observatory, Columbia University, Palisades, 10964, USA
[d] NASA Goddard Institute for Space Studies, New York, 10025, USA
[e] Department of Computer Science, Columbia University, New York, 10027, USA
[f] School of Engineering and Applied Sciences, Harvard University, Cambridge, 02138, USA
[g] Department of Earth and Planetary Sciences, Harvard University, Cambridge, 02138, USA

GRAPHICAL ABSTRACT

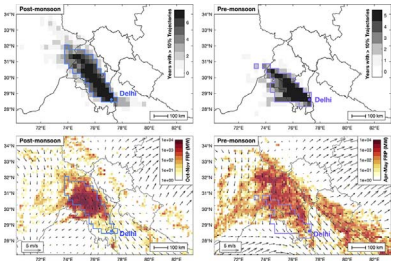

ARTICLE INFO

Keywords:
Air quality
Outdoor fires
Crop residue burning
HYSPLIT
India

ABSTRACT

Air pollution in many of India's cities exceeds national and international standards, and effective pollution control strategies require knowledge of the sources that contribute to air pollution and their spatiotemporal variability. In this study, we examine the influence of a single pollution source, outdoor biomass burning, on particulate matter (PM) concentrations, surface visibility, and aerosol optical depth (AOD) from 2007 to 2013 in three of the most populous Indian cities. We define the upwind regions, or "airsheds," for the cities by using atmospheric back trajectories from the HYSPLIT model. Using satellite fire radiative power (FRP) observations as a measure of fire activity, we target pre-monsoon and post-monsoon fires upwind of the Delhi National Capital Region and pre-monsoon fires surrounding Bengaluru and Pune. We find varying contributions of outdoor fires to different air quality metrics. For the post-monsoon burning season, we find that a subset of local meteorological variables (air temperature, humidity, sea level pressure, wind speed and direction) and FRP as the only pollution source explained 39% of variance in Delhi station PM_{10} anomalies, 77% in visibility, and 30% in satellite AOD; additionally, per unit increase in FRP within the daily airshed (1000 MW), PM_{10} increases by 16.34 μg m^{-3}, visibility decreases by 0.155 km, and satellite AOD increases by 0.07. In contrast, for the pre-monsoon burning season, we find less significant contributions from FRP to air quality in all three cities. Further, we attribute 99% of FRP from post-monsoon outdoor fires within Delhi's average airshed to agricultural burning. Our work suggests that although outdoor fires are not the dominant air pollution source in India throughout the year, post-monsoon fires contribute substantially to regional air pollution and high levels of population exposure around Delhi. During 3-day blocks of extreme $PM_{2.5}$ in the 2013 post-monsoon burning season, which coincided

* Corresponding author.
E-mail address: tianjia.liu@columbia.edu (T. Liu).

http://dx.doi.org/10.1016/j.atmosenv.2017.10.024
Received 14 May 2017; Received in revised form 20 September 2017; Accepted 9 October 2017
Available online 02 November 2017

with statistically significant high fire activity, concentrations in Delhi averaged 304 μg m^{-3}, or more than 1000% above the 24-h $PM_{2.5}$ guideline (25 μg m^{-3}) of the World Health Organization. These results suggest that providing viable alternatives to agricultural residue burning could help improve post-monsoon air quality for a growing population of 63 million (39% in urban areas) within Delhi's airshed.

1. Introduction

More than half of the Indian Subcontinent's population is exposed to average annual fine particulate matter (diameter less than 2.5 μm; $PM_{2.5}$) concentrations that surpass the least stringent annual $PM_{2.5}$ guideline (35 μg m^{-3}) of the World Health Organization (WHO); mean annual $PM_{2.5}$ in 49% of the subcontinent's inhabited area exceeds the most stringent 10 μg m^{-3} guideline (Dey et al., 2012; WHO, 2006). Recent global air pollution studies highlight the public health importance of improving air quality in India, where approximately 600,000 annual premature deaths are attributable to outdoor air pollution, ranking second only to China (Lelieveld et al., 2015; Ghude et al., 2016; WHO, 2016). $PM_{2.5}$ exposure is associated with an average lost life expectancy of 3.4 years across the country and up to 6.4 years in Delhi (Ghude et al., 2016). Air pollution in India is a growing threat to public health, especially in high-density population centers exposed to high concentrations of particulate matter.

Controlling air pollution in India is challenging because of complex interactions between local and regional sources (Kumar et al., 2015a). Due to atmospheric transport, areas with higher aerosol emissions do not always correspond to higher aerosol concentrations (Kishcha et al., 2014). Across the country, the most common anthropogenic emissions sources are from vehicles, manufacturing, electricity generation, construction and road dust, waste burning, and household energy use (Guttikunda et al., 2014; CPCB, 2011, Gargava and Rajagopalan, 2015a; 2015b; Sharma and Dikshit, 2016). Even single sources can have large health impacts. For example, emissions from coal-fired power plants have increased by 70% since the mid-1990s (Lu and Streets, 2012), and 111 coal-fired power plants across the country were linked to an estimated 80,000–115,000 premature deaths due to $PM_{2.5}$ exposure in 2010–2011 (Guttikunda and Jawahar, 2014). Despite implementation of different air quality policies, population growth, increasing living standards, and the concomitant demand for transportation, energy, and industry have contributed to increasing PM pollution levels over the past decade (Gurjar et al., 2016; CPCB, 2012). Rising emissions, especially when coupled with population growth, are expected to increase the future burden of population exposure to air pollution (Lelieveld et al., 2015; Guttikunda and Jawahar, 2014), underscoring the need to better understand how different sources impact air pollution.

Several previous studies have examined air quality in Delhi National Capital Region (NCR; hereafter referred to as Delhi). During 2007–2008, more than two-thirds of $PM_{2.5}$ samples exceeded the national ambient air quality 24-h standard of 60 μg m^{-3} (Tiwari et al., 2013; CPCB, 2009), with the highest exposure in the winter when atmospheric conditions are typically more stable and surface ventilation is weak (Tiwari et al., 2013, 2014a). In Delhi, previous efforts to control pollution in the early 2000s, such as converting all commercial vehicles to compressed natural gas and closing polluting industries, helped to improve respiratory health (Foster and Kumar, 2011), but these gains may be now overshadowed by the increased vehicle population (Gurjar et al., 2016). Air pollution studies in other Indian cities are more limited, but also consistently show significant exceedances of air pollutant concentrations over national and international standards. In 2010, annual average PM_{10} concentrations in six Indian cities (Pune, Chennai, Indore, Ahmedabad, Surat, and Rajkot) ranged from 73 to 119 μg m^{-3}, all above the national standard and corresponding to 15,200 premature deaths per year, with contributions from industrial activities, transportation, and road dust (Guttikunda and Jawahar, 2012).

In addition to the contributions of urban sources to air quality degradation, outdoor fires are a regional air pollution source dominated by fires in agricultural regions (Vadrevu et al., 2008). Particularly in northern India, fires are mostly from residue burning, which peaks in April to May (pre-monsoon) and October to November (post-monsoon), corresponding to burning after the wheat and rice harvests, respectively (Vadrevu et al., 2011; Venkataraman et al., 2006). In the region of Punjab, mechanized harvesting has reduced the need for manual labor in the past two to three decades. However, the scattered, root-bound crop residue left behind by combine harvesters is difficult to remove, and burning is usually the fastest and cheapest method to clear fields for the next planting (Gadde et al., 2009; Kumar et al., 2015b). An estimated 7–8 million tonnes of rice residue associated with post-monsoon agricultural burning are burned each year in Punjab, India (Kumar et al., 2015b).

Wheat and rice residue burning releases accumulation mode aerosols that mostly contribute to the $PM_{2.5}$ fraction (Hays et al., 2005). Post-monsoon burning lasts for several weeks and is associated with increased AOD across the Indo-Gangetic Plains (IGP); in contrast, pre-monsoon fires are not the dominant contributor to air quality degradation (Vadrevu et al., 2011; Singh and Kaskaoutis, 2014). Atmospheric trajectory analysis shows aerosol plumes traveling eastward from northwestern India across the IGP (Kaskaoutis et al., 2014; Vijayakumar et al., 2016; Mishra et al, 2012). Satellite-based studies of post-monsoon burning in the Indo-Gangetic Basin (IGB) have shown elevated layers of aerosols from the surface to 4–4.5 km altitude, with peak concentrations below 1 km (Mishra and Shibata, 2012). Ground measurements in northwestern India also show increases in aerosol, SO_2, and NO_2 concentrations during rice and wheat burning periods (Mittal et al., 2009).

In this study, we investigate the contribution of a single pollution source, outdoor biomass burning, to PM concentrations (as well as surface visibility and AOD) from 2007 to 2013 in three of India's populous cities (Delhi, Bengaluru, and Pune) by combining satellite fire observations, atmospheric trajectory modeling, and ground and satellite-based air quality observations. We focus on these three cities because they consistently had the highest fire activity in their surroundings relative to other major cities. We specifically address the following questions: 1) In which of the three Indian cities considered in this study are PM concentrations most affected by outdoor fires in their surroundings; 2) In which seasons do outdoor fires upwind of the three Indian cities most strongly affect PM concentrations through transport of emissions to cities; 3) To what extent are PM concentrations from outdoor burning in airsheds of India cities attributable to agricultural burning versus other fire types; and 4) How many people are exposed to degraded air quality from outdoor fires in the airsheds in these Indian cities?

2. Data and methods

2.1. Fire activity

We quantify fire activity with MODIS daily maximum fire radiative power (FRP) observations over India from January 2007 to December 2013. MODIS FRP estimates the amount of energy released by a fire (Wooster et al., 2005) and has been previously used to estimate variability in fire activity over time and by land cover type in India (Vadrevu et al., 2013). Data are from Collection 6 Aqua (MYD14A1) and Terra (MOD14A1) products (http://reverb.echo.nasa.gov),

available at 1 km^2 spatial resolution. We use these observations to quantify the spatiotemporal dynamics of fires across India within 200 km radii for the 10 most populous cities. The selection of 200 km is based on an initial estimate of the travel distance of carbonaceous aerosols, whose approximate atmospheric lifetime is 1–6 days (Pan et al., 2013). We further refine the travel distance and transport pathways through analysis of atmospheric trajectories (Section 2.2).

2.2. HYSPLIT trajectory modeling

We use the National Oceanic and Atmospheric Administration (NOAA) Air Resource Laboratory's (ARL) Hybrid Single-Particle Lagrangian Integrated Trajectory model (HYSPLIT) (Stein et al., 2015; Rolph, 2016) to measure the influence of burning emissions within the "airsheds" of three major Indian cities that are most affected by fires: Delhi, Bengaluru, and Pune. We hereafter use the term "airshed" to refer to the spatial zone around a city where emissions can contribute to pollution within that city (in this case, due to outdoor fires).

Previous studies have used HYSPLIT back trajectories to monitor the influence of fires on air quality in nearby locations, both in India (Badarinath et al., 2009; Beegum et al., 2009; Mishra and Shibata, 2012; Safai et al., 2007; Tiwari et al., 2014b) and other locations around the world (Sahani et al., 2014; Sapkota et al., 2005; Atwood et al., 2013; Dotse et al., 2016; Kusumaningtyas and Aldrian, 2016; Miller et al., 2011; Cady-Pereira et al., 2017). We start 72-h HYSPLIT back trajectories from Delhi (28.62° N, 77.21° E), Bengaluru (12.97° N, 77.57° E), and Pune (18.52° N, 73.86° E) at 4:30 p.m. local time, approximating the 1–6 day lifetime of organic and elemental carbon aerosols (Pan et al., 2013) and the peak time of regional burning (Giglio, 2007), respectively (Table S1). Meteorology is from the NCEP Global Data Assimilation System (GDAS) model at 0.5° × 0.5° spatial resolution, available since September 2007.

The starting heights selected for back trajectory analysis in previous studies range from 100 m to more than 4 km above the receptor location, but those focused specifically on agricultural burning in India tend to use lower starting heights, generally below ~2 km (Badarinath et al., 2009; Beegum et al., 2009; Mishra and Shibata, 2012; Safai et al., 2007). Thus, we run back trajectories at three altitudes: 500 m, 1 km, and 1.5 km. To then select the altitudes to be used for further analysis for each city and burning season, we estimate the planetary boundary layer (PBL) height, which is characterized by turbulent flow and strong vertical mixing, using the 2007–2012 MERRA meteorological fields at 2° × 2.5° (latitude by longitude) spatial resolution with 47 vertical layers (Rienecker et al., 2011). The average PBL heights for each city and season in 2007–2012 are as follows: 437 m for Delhi post-monsoon, 1441 m for Delhi pre-monsoon, 864 m for Bengaluru pre-monsoon, and 837 m for Pune pre-monsoon (Fig. S4). Using MERRA PBL heights as a guide, we choose starting heights of the HYSPLIT trajectories that were near or below the PBL height. We use the following trajectory heights for each city and burning season: 500 m for Delhi post-monsoon, 500 m, 1 km, and 1.5 km for Delhi pre-monsoon, and 500 m for Bengaluru and Pune pre-monsoon.

We construct airsheds at two temporal resolutions: daily and seasonal (two-month period). We use daily airsheds for statistical analyses of air quality observations (Sections 2.4), seasonal airsheds to analyze the sources of outdoor fires (Section 2.5), and composite (average multi-annual) seasonal airsheds to characterize fire intensity, surface winds, and population-level exposure (Section 2.3).

2.2.1. Daily airsheds

In order to extract fires within the airsheds around the three cities, we consider a 10 km buffer (20 km total width) around the HYSPLIT trajectories. While this buffer size is somewhat arbitrary, we do not find significant differences when we looked at a 5 km buffer (data not shown). We account for the lag in travel time from FRP source regions to the three cities by grouping the hourly output coordinates from HYSPLIT atmospheric trajectories by day (Fig. 1). We then extract the total FRP within the HYSPLIT trajectory buffers based on this spatial and temporal information. We use the aggregate FRP within the daily airshed, which often cover more than 50 MODIS pixels, including the 10 km buffer around the trajectories to mitigate FRP uncertainties (Freeborn et al., 2014).

2.2.2. Seasonal airsheds

We construct seasonal airsheds for each burning season and city. We rasterize all daily trajectories at the selected altitudes according to a 0.3° × 0.3° resolution grid centered on each city. Each pixel that a trajectory intersects is assigned a value of 1. The density of groups of individual trajectories can be spatially approximated as a ratio to total trajectories. We then take pixels with a density > 0.1 to represent the seasonal airshed of a given year. To construct a composite airshed that spans the years of study and accounts for interannual variability, the

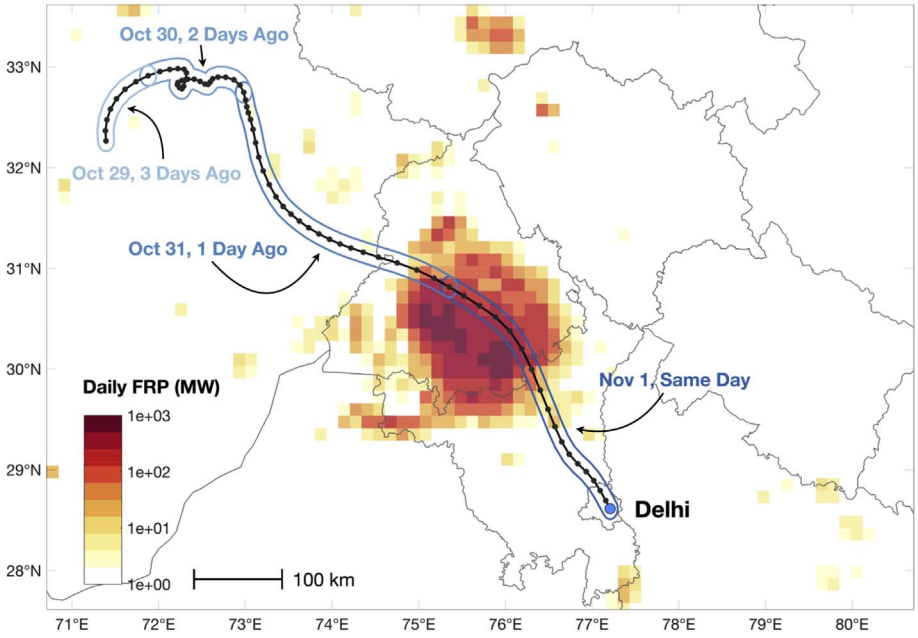

Fig. 1. Example of daily Delhi airshed for November 1, 2007. This 72-h HYSPLIT back trajectory (black line, with hourly coordinates) started from Delhi at 500 m height spans 4 days from October 29 to November 1. The daily airshed (blue), defined as the 10-km buffer of the back trajectory, is separated into 4 days to extract and sum the FRP for each day. The average 4-day FRP (MW, in logarithmic scale) shown above is aggregated to 15 km × 15 km spatial resolution. (For interpretation of the references to colour in this figure legend, the reader is referred to the web version of this article.)

seasonal trajectory density maps are averaged across years, again constraining to pixels with a density > 0.1 (Fig. 2 and Fig. S1).

2.3. Air quality, population, and wind speed data

Due to the respective limitations of available air quality datasets, we use several satellite and ground-based data sources to assess air quality in each city, as described below:

1) PM_{10}: We downloaded station data from India's Central Pollution Control Board (CPCB) National Ambient Air Quality Monitoring (NAMP) Network (CPCB, 2012). We use all available stations for Delhi, Bengaluru, and Pune from CPCB's Environmental Data Bank (http://cpcb.nic.in/; Table S2), but significant gaps exist in data availability per station and per month. Previous studies show considerable day-to-day variability in independent daily PM measurements in Delhi, and thus point to the lack of reliability in CPCB data (Tiwari et al., 2014b; Bisht et al., 2016). However, for each city, CPCB observations are often recorded at multiple stations and overall span a longer time period (Table S2). While observations are limited to approximately 6–9 days per month and per station, they do not usually overlap among the different stations of each city. We thus account for the data sparseness of individual stations by normalizing PM_{10} among all stations within a city to produce a citywide average PM_{10} anomaly record. Due to PM_{10} biases among industrial and residential stations, we focus on the relative PM_{10} difference from the mean rather than absolute PM_{10} values. We calculate the PM_{10} anomaly based on the difference between PM_{10} observations and the mean 2007–2013 PM_{10} for each station. The individual station PM_{10} anomalies are then averaged per day to produce a citywide average.
2) $PM_{2.5}$: Although available for a shorter time period than the CPCB dataset, the U.S. Embassy in Delhi has monitored daily $PM_{2.5}$ concentrations since 2013 (http://newdelhi.usembassy.gov/airqualitydata.html).
3) Visibility: Visibility measurements are from the National Climatic Data Centre (NCDC) Global Summary of the Day (GSOD) (https://www.ncdc.noaa.gov/isd/products). While not a direct measure of air quality, degraded visibility is associated with increased air pollution as it measures the surface visual range, or ability to detect an object's outline against the horizon, as typically reported by a human observer from airport towers (WMO, 1996). We downloaded all available records for Delhi and Bengaluru and average the daily measurements across stations (Table S3).
4) Ground-based AOD: AERONET (AErosol RObotic NETwork) Level 2.0 quality assured observations (Holben et al., 1998) are available for Pune (18.54° N, 73.81° E) at the 440 nm, 675 nm, 870 nm, and 1020 nm wavelengths; we use the observations at the 440 nm wavelength (http://aeronet.gsfc.nasa.gov/new_web/data.html) (Table S4).
5) Satellite AOD: We use the daily 1° × 1° (latitude by longitude) spatial resolution product from MODIS Collection 6 Level 3 Aqua deep blue and dark target combined retrieval (MYD08D3) (Levy et al., 2013). We extract daily AOD (550 nm wavelength) from the pixels corresponding to each city.
6) Population: In order to estimate the human population affected by outdoor burning, we use the 2010 UN-adjusted Gridded Population of the World (GPW), version 4 population count (CIESIN, 2016). GPWv4 (30 arc-second resolution) is a globally integrated dataset constructed from the extrapolation of raw population and housing census counts in national and sub-national administrative units (Fig. S2). The UN-adjusted GPWv4 dataset adjusts for the 2015 UN World Population Prospects national population estimates. Urban populations within airsheds of Delhi, Bengaluru, and Pune were estimated by using MODIS-derived dataset from Schneider et al. (2010).
7) Surface winds: For the characterization of average surface wind patterns, we use the Cross-Calibrated Multi Platform (CCMP) wind vector analysis product, version 2 (Wentz et al., 2015). The Level 3 product incorporates satellite, moored buoy, and model wind data to produce high resolution 0.25° × 0.25° gridded surface vector winds at 10 m above surface (Remote Sensing Systems; http://www.remss.com).

2.4. Statistical analysis

2.4.1. Best subset regression

We assess the influence of fires within the daily airsheds of the three cities on the different measures of air quality while controlling for local meteorology (from wunderground.com). We use best subset regression to generate the best 1 to *n*-variable linear regression models by selectively incorporating predictors from: 1) FRP within the daily airshed and 2) local meteorological variables (air temperature, relative humidity, dew point temperature, sea level pressure, wind speed, and wind direction). The advantages of using a subset of available variables include eliminating uninformative variables and reducing the standard errors of estimated regression coefficients (Miller, 1984). We then use the Bayesian Information Criterion (BIC), which incorporates a more stringent size penalty than the Akaike Information Criterion (AIC) and thus favors simpler models, to select the final model (Schwarz, 1978). Using best subset regression and BIC as the objective criterion, we can focus on the most meaningful explanatory variables and determine whether FRP within the daily airshed is an important predictor of variance in air quality observations.

We consider coarser temporal resolutions with 3-day, 5-day, and 7-day averaging windows rather than simply using daily observations due to uncertainties in missing PM_{10} and ground-based AOD data and in FRP (Freeborn et al., 2014). Since we find close agreement between the three averaging windows, we select the 5-day model as representative of potential short-term and long-term pollution effects. We use a "block" mean, which averages *n* values every *n* days, according to the averaging window size *n*. We use the block mean rather than the rolling mean (moving average) in order to avoid artificially strengthening correlation and increasing the sample size. All data are detrended to remove systematic shifts and focus on daily fluctuations in the data. However, data are not deseasonalized, since only sub-seasonal (two month) timeframes are considered. We also exclude predictors with a variance inflation factor (VIF) > 5, which is a more stringent threshold than 10, the general rule of thumb for identifying severe multiple collinearity where independent variables are correlated (Menard, 2002; Kutner et al., 2004).

2.4.2. Extreme pollution days

We perform two-sample Welch t-tests on FRP within the daily airshed for extreme and normal days as defined for each air quality metric. Extreme pollution days during a burning season are characterized as 1 standard deviation above the mean for station PM_{10} anomaly, station $PM_{2.5}$, satellite AOD and ground-based AOD, and 1 standard deviation below the mean for visibility. Normal pollution days represent days not defined as extreme pollution days for that metric.

2.5. Crop and land cover

We use the University of Maryland (UMD) scheme of the yearly 500 m × 500 m MODIS MCD12Q1 Land Cover Type product (Collection 5) to attribute total FRP within the seasonal airshed to land cover categories. We simplify the UMD scheme classes to six classes: cropland, forest, shrubland, grassland, and savanna, barren and sparse vegetation, urban and built-up, and unclassified.

In addition, monsoon crops, most often rice, are the main agricultural crop throughout India. Farmers grow a second crop in the winter, often wheat or pulses, where water is available (Mondal et al., 2015). For the post-monsoon burning season, we apply a second land

cover classification scheme using the India cropped area dataset from Jain et al. (2013, 2017). This MODIS-based dataset estimates the percentage of winter cropped area annually from the 2000–01 to 2015–16 winter crop season and uses a forest mask derived from Hansen et al. (2013). We categorize land cover within the post-monsoon airshed as quintiles of winter crop (ranging from 0 to 100%), forest, and other (non-agricultural and non-forest).

3. Results

3.1. Fires within a radius of 200 km

To select our cities of interest, we extract the total monthly FRP within a 200 km radius around the 10 most populous Indian cities (Fig. S3). The 200 km radius around Delhi has the highest 2007–2013 average total annual FRP of 2.3E + 05 MW. The Pune, Mumbai, and Bengaluru annual averages are ranked second, third, and fourth with 7.2E + 04 MW, 5.5E + 04 MW, and 5.4E + 04 MW, respectively. However, because the Pune and Mumbai radial airsheds share a 56% overlap in area and Mumbai only averages slightly higher annual FRP than Bengaluru, we choose Bengaluru as our third city. Different seasonal dynamics are also evident. In Delhi, fire intensity in the 200 km radius peaks in October and then again in April to May. The peak in Pune is from March to April and in Bengaluru, from February to March. We also explore different radii from 100 to 300 km; since Delhi, Pune, and Bengaluru have high fire activity most consistently from 2007 to 2013, we select these three cities for further analysis.

3.2. Fires within HYSPLIT-derived airsheds

Unlike the static 200 km radial airsheds used for initial assessment, HYSPLIT-derived airsheds vary spatially and temporally in the three cities for a subset of the three altitudes: 500 m, 1 km, and 1.5 km (described in Section 2.2). For every year, we define the fire season for each city airshed as two months with peak burning (Table S1): 1) October to November for Delhi post-monsoon burning; 2) April to May for Delhi pre-monsoon burning; 3) February to March for Bengaluru pre-monsoon burning; 4) March to April for Pune pre-monsoon burning. The two peak months represent repeated and sustained fire activity with high FRP (Fig. S5). Outdoor burning in Delhi's airsheds is the most intense (FRP > 500 MW) and sustained from the last 2–3 weeks of October through the first two weeks of November (post-monsoon) and from the last week of April through the first 3 weeks of May (pre-monsoon) (Figs. S5a–b). In contrast, outdoor fires within the airsheds of Bengaluru and Pune during the pre-monsoon burning seasons are usually characterized by low FRP (< 500 MW) and relatively shorter (sub-weekly), interannually variable, and discontinuous events (Figs. S5c–d).

3.2.1. Delhi

Delhi's pre-monsoon and post-monsoon airsheds are characterized by high fire intensity and relatively weak northwesterly winds (Fig. 2). The average post-monsoon Delhi airshed, extending northwest to Haryana and Punjab and across the border to Pakistan, comprises a population of 63 million (39% in urban areas) (Fig. S2). In contrast, the

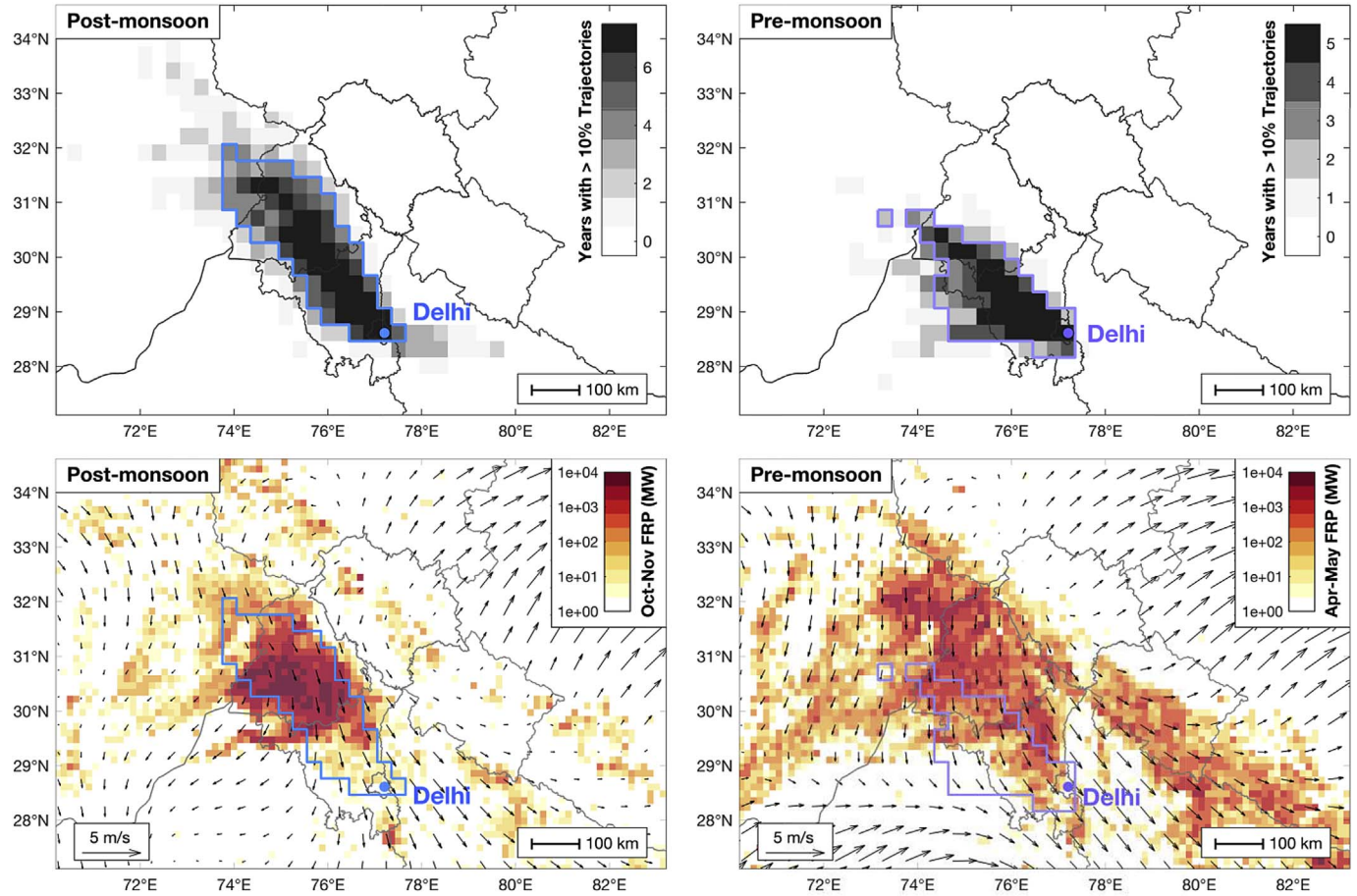

Fig. 2. Delhi composite post-monsoon and pre-monsoon airsheds, total season FRP, and average winds. The composite post-monsoon (blue) and pre-monsoon (purple) airsheds are approximated from the intersection of more than 10% of total HYSPLIT back trajectories with 0.3° × 0.3° pixels. The top panels show the interannual variability of seasonal airsheds depicted in shades of gray; darker colors represent a high number of years with back trajectories passing through that location. The bottom panels show the average seasonal FRP (MW, in logarithmic scale) aggregated to 15 km × 15 km spatial resolution. Average seasonal surface winds at 10 m above surface are averaged to 0.5° × 0.5° spatial resolution. (For interpretation of the references to colour in this figure legend, the reader is referred to the web version of this article.)

average pre-monsoon Delhi airshed extends less to the northwest and more to the south, covering only Haryana and southern Punjab. The average post-monsoon Delhi airshed comprises a smaller population of 39 million (48% in urban areas).

In Delhi's pre-monsoon and post-monsoon airsheds, fire activity occurs primarily on cropland. On average, pre-monsoon and post-monsoon agricultural fires are associated with 99% of total FRP within the seasonal airshed; in terms of area, the post-monsoon airshed averages 96% cropland, 4% urban and built-up, and 1% grassland, shrubland, and savanna, and the pre-monsoon airshed averages 83% cropland, 13% grassland, shrubland, and savanna, and 3% urban and built-up (Fig. 3). Moreover, according to the Jain et al. (2013, 2017) winter crop dataset, the contribution to FRP increases with % area winter crop: the 1-km^2 pixels with the highest FRP in the post-monsoon burning season are associated with those with higher winter crop cover (Fig. S7). During the post-monsoon burning seasons from 2007 to 2013, FRP within the seasonal airshed is dominated by fires in pixels 80–100% covered by winter crop. The 80–100% winter crop percentile contributes on average 78% of total FRP and 45% of total area within the post-monsoon seasonal airshed. Thus, the land cleared of monsoon crop residue during post-monsoon burning is linked to the land used to subsequently sow the winter crop.

FRP within the daily airshed is generally not well correlated with air quality observations, except for moderately with visibility during the post-monsoon burning season and station PM_{10} anomaly during both burning seasons (Fig. 4, S5a–b; Tables S6a–b). In post-monsoon, peaks in FRP within the daily airshed correlate with high mean PM_{10} anomaly and $PM_{2.5}$, low visibility, and high satellite AOD; in contrast, such correlation of FRP within the daily airshed with air quality metrics is not observed pre-monsoon (Figs. S5a–b). The 5-day FRP and local meteorology models explain 39% of variance in average station PM_{10} anomaly, 77% in visibility, and 30% in satellite AOD (Table 1). According to the 5-day models, PM_{10} increases by 16.34 μg m^{-3}, visibility decreases by 0.155 km, and satellite AOD increases by 0.07 per unit increase in FRP (1000 MW). In contrast, for pre-monsoon burning, FRP within the airshed is not selected as a skillful predictor by best subset regression in any of the three final 5-day air quality models. Rather, local meteorology alone, with minimum temperature and humidity in particular, is more helpful in explaining variance in pre-monsoon air quality observations. The pre-monsoon 5-day local-meteorology-only models indicate that minimum temperature and minimum humidity together explain 40% of variance in station PM_{10} anomaly and 35% in satellite AOD, while mean wind speed alone explains 8% of variance in visibility.

In addition, we find that the difference between FRP within the daily airshed in extreme and normal pollution days during the post-monsoon burning season for Delhi's airshed is statistically significant (p-value $<$ 0.05) for all averaging windows for station PM_{10} and $PM_{2.5}$ and for the 3-day averaging window for visibility (Table S8). For the 5-day averaging window, FRP within the airshed averages 2014 MW on extreme PM_{10} anomaly (176 μg m^{-3}) days and 804 MW on normal PM_{10} anomaly (25 μg m^{-3}) days. For the 3-day averaging window, FRP within the airshed averages 4822 MW on extreme $PM_{2.5}$ (304 μg m^{-3}) days and 993 MW on normal $PM_{2.5}$ (147 μg m^{-3}) days in 2013. In contrast, we do not find that FRP within the airshed on extreme versus normal pollution days are statistically significantly different during the

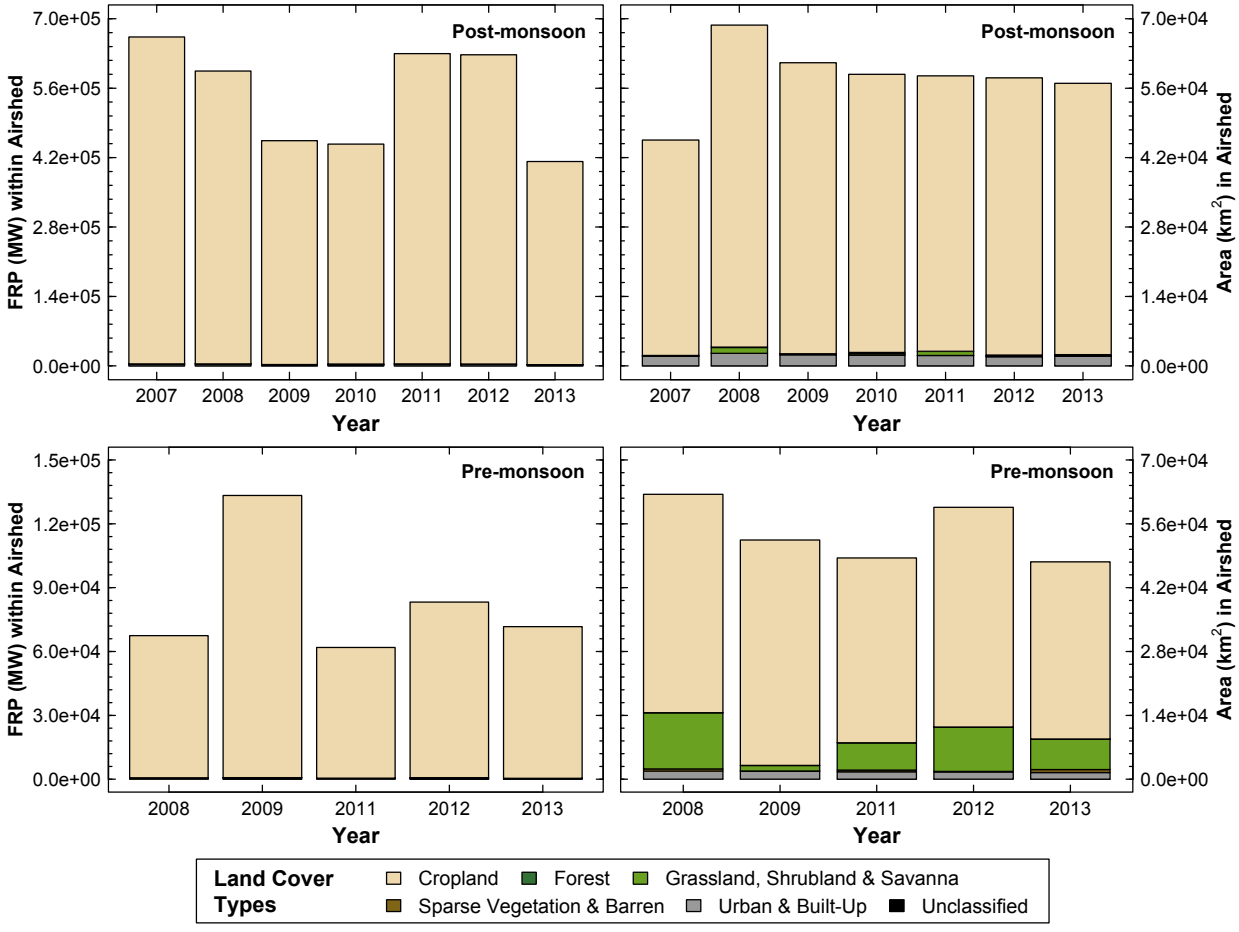

Fig. 3. Annual FRP and area by simplified MCD12Q1 land cover types in Delhi post-monsoon and pre-monsoon airsheds. The top panels show the FRP contribution and total area for each land cover class within the 2007–2013 post-monsoon airsheds. The bottom panels show the FRP contribution and total area for each land cover class within the 2008–2009 and 2011–2013 pre-monsoon airsheds.

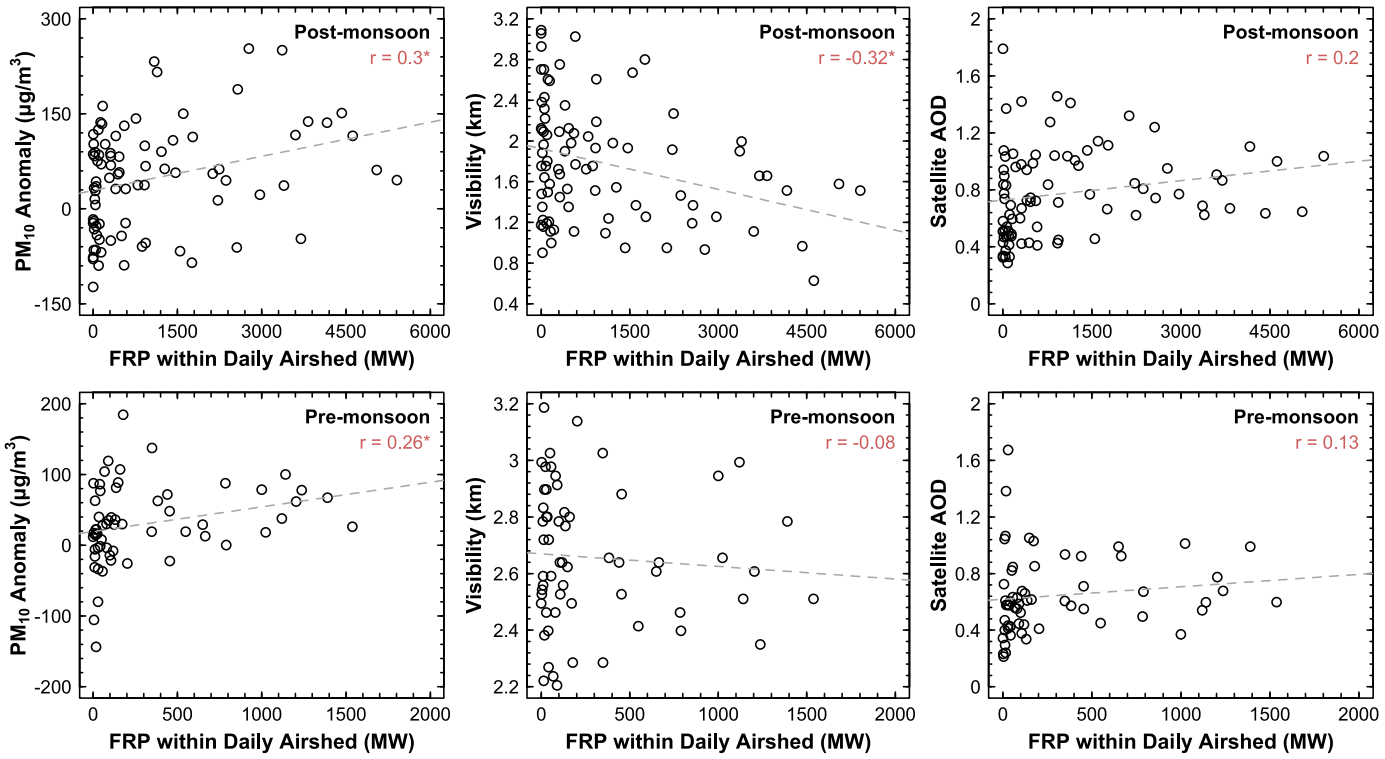

Fig. 4. Correlations between FRP within the daily Delhi airshed (MW) and local Delhi air quality observations (PM_{10} anomaly, visibility, and satellite AOD). The top panels depict scatterplots for the 5-day averaging window for the post-monsoon burning season, and the bottom panels depict those for the pre-monsoon burning season. Starred correlations are statistically significant (p-value $<$ 0.05).

Table 1
FRP and local meteorology regression models of Delhi post-monsoon and pre-monsoon air quality for the 5-day averaging window. FRP refers to the total FRP within the daily Delhi airshed; meteorological variables are from local observations at Indira Gandhi International Airport (DEL). For wind direction in degrees, 0 = North, 90 = East, 180 = South, and 270 = West. Detrended variables for the final multiple linear regression models are selected from best subset regression and BIC. Meteorological variables uninformative to the regression models are not shown. The statistical significance (based on p-values) of the regression coefficients is denoted as follows: 0–0.001 '***', 0.001–0.01 '**', 0.01–0.05 '*', 0.05–0.1 ''. Standard errors of the regression coefficients are shown in parentheses.

Predictors	PM_{10} Anomaly		Visibility		Satellite AOD	
	Post-monsoon	Pre-monsoon	Post-monsoon	Pre-monsoon	Post-monsoon	Pre-monsoon
Ordinary R^2	0.42	0.42	0.79	0.1	0.34	0.37
Adjusted R^2	0.39	0.4	0.77	0.08	0.3	0.35
FRP (1000 MW)	16.34**	–	−0.155***	–	0.07**	–
	(5.32)		(0.024)		(0.02)	
Min Temp (°C)	–	3.75*	–	–	–	0.043***
		(1.84)				(0.01)
Max Temp (°C)	−8.05**	–	0.046**	–	0.054***	–
	(2.47)		(0.015)		(0.014)	
Min Humidity (%)	–	−4.36***	–	–	–	0.022***
		(0.83)				(0.004)
Max Humidity (%)	–	–	−0.019***	–	0.012**	–
			(0.005)		(0.004)	
Max Sea Level Pressure (hPa)	–	–	−0.066***	–	0.042**	–
			(0.017)		(0.015)	
Mean Wind Speed (km h^{-1})	−3.61*	–	0.109***	0.039*	–	–
	(1.55)		(0.019)	(0.016)		
Max Wind Speed (km h^{-1})	−11.66*	–	–	–	–	–
	(4.61)					
Wind Direction (degrees)	–	–	0.002**	–	−0.002***	–
			(0.001)		(0.001)	

pre-monsoon burning season for Delhi's airshed.

3.2.2. Bengaluru

Bengaluru's pre-monsoon airshed extends eastward across Tamil Nadu and Andhra Pradesh and is characterized by low fire intensity and relatively strong easterly winds from the Bay of Bengal (Fig. S1). The composite Bengaluru pre-monsoon airshed comprises a population of 37 million (29% in urban areas) (Fig. S2).

Fire activity within Bengaluru's pre-monsoon airshed occurs primarily on cropland, forest, and grassland, shrubland, and savanna. On average, fires on cropland contribute 64% to total FRP, while those in forest area and grassland, shrubland, and savanna contribute 26% and

9%, respectively, to total FRP (Fig. S8). Moreover, Bengaluru's pre-monsoon airshed averages 76% cropland, 17% grassland, shrubland, and savanna, 5% forest, and 2% urban and built-up in area (Figs. S6 and S8). FRP within the daily airshed is positively correlated with station PM_{10} anomaly and visibility; the latter is unexpected, since visibility generally decreases with higher fire activity (Figs. S5c and S9; Table S6c). Correlations between FRP within the daily airshed and satellite AOD are not statistically significant. Moreover, FRP within the airshed is not selected by best subset regression as a skillful predictor in any of the 5-day models of air quality (Table S5a). The 5-day local meteorology only models explain 39% of variance in station PM_{10} anomaly, 53% in visibility, and 30% in satellite AOD. The station PM_{10} anomaly model uses maximum humidity, the visibility model uses minimum dew point temperature, mean and maximum wind speed, and wind direction, and the satellite AOD model uses maximum temperature and minimum dew point temperature as explanatory variables. Moreover, we do not find that extreme and normal pollution days are statistically significantly different during the pre-monsoon burning season for Bengaluru's airshed.

3.2.3. Pune

Pune's pre-monsoon airshed extends northwestward in Maharashtra and is characterized by low fire intensity and relatively strong northwesterly winds from the Arabian Sea (Fig. S1). The composite Pune pre-monsoon airshed comprises a population of 34 million (55% in urban areas) (Fig. S2).

Fire activity within Pune's pre-monsoon airshed occurs primarily on grassland, shrubland, and savanna and cropland. On average, fires on grassland, shrubland, and savanna contribute 47% to total FRP, and those on cropland contribute 46% to total FRP (Fig. S8). Moreover, Pune's pre-monsoon airshed averages 63% cropland, 29% grassland, shrubland, and savanna, 4% forest, 4% urban and built-up, and 1% barren and sparse vegetation in area (Figs. S6 and S8). Correlations between FRP within the daily airshed and air quality metrics are not statistically significant (Figs. S5d and S9; Table S6d). Moreover, FRP is not selected by best subset regression as a skillful predictor in any of the 5-day models of air quality (Table S5b). The 5-day local meteorology models explain 24% of variance in station PM_{10} anomaly, 18% in visibility, and 48% in satellite AOD. The station PM_{10} anomaly model uses minimum temperature and maximum humidity, the ground-based AOD model uses minimum dew point and mean wind speed, and the satellite AOD model uses maximum temperature and minimum dew point as explanatory variables. We also do not find that extreme and normal pollution days are statistically significantly different for Pune's airshed.

4. Discussion and conclusions

Air pollution is a critical public health issue; India's population (currently 1.31 billion) is expected to grow to 1.7 billion by 2050 (United Nations, 2015). Both its urban and rural populations are increasingly vulnerable to degraded air quality from agricultural residue burning (Kumar et al., 2015b). We focus on outdoor biomass burning to identify the contributions from this source in the context of the many other sources, including vehicles, power plants, waste burning and industries. In this paper, we present a method of using HYSPLIT back trajectories to approximate daily and seasonal city airsheds in order to assess the impact of regional outdoor biomass burning to air quality in three populous Indian cities with the most consistent occurrence of fires in close proximity: Delhi, Pune, and Bengaluru.

We initially select the three cities of this study based on annual FRP within a radius of 200 km. However, airsheds constructed from 72-h HYSPLIT back trajectories show that airsheds are not equidistantly distributed around a city, but instead dynamically change both seasonally and annually, with trajectories often concentrated in one direction and extending beyond a 200 km radius. For example, the post-monsoon Delhi airshed extends to the northwest to Haryana and Punjab, while the pre-monsoon Delhi airshed lies more to the south and only covers southern Punjab and Haryana. The post-monsoon Delhi airshed is characterized by relatively high fire intensity due to: 1) higher overall FRP during the post-monsoon burning season, and 2) the extension of HYSPLIT-derived airsheds into Punjab, a state with high FRP density during both burning seasons.

We find that although outdoor fires within the Delhi airshed occur both post-monsoon (October to November) and pre-monsoon (April to May), post-monsoon fires, 99% of which were located in agricultural areas, are more likely to impact Delhi's air quality. Best subset regression selects FRP within the daily airshed, in addition to local meteorological variables, as a skillful predictor of variance in post-monsoon Delhi air quality in all three 5-day regression models, but in none of the models for pre-monsoon Delhi air quality. The three post-monsoon 5-day models, using local meteorological variables and FRP within the daily airshed as the only pollution source, explain 39% of variance in average station PM_{10} anomaly, 77% in visibility, and 30% in satellite AOD, respectively; for per unit increase in FRP (1000 MW) within the airshed, PM_{10} increases by 16.34 $\mu g\ m^{-3}$, visibility decreases by 0.155 km, and satellite AOD increases by 0.07. Post-monsoon, the combination of higher overall FRP in northwestern India and lower boundary layer from weather patterns characterized by cooler temperatures, higher relative humidity, and weaker winds favors the transport of pollutants into Delhi and deterioration of Delhi's air quality from agricultural fires (Singh and Kaskaoutis, 2014). We find that the regression coefficients of the explanatory local meteorological variables in the 5-day regression models mostly corroborate these findings. For example, the negative coefficients of the maximum temperature and mean and maximum wind speed variables in the PM_{10} model suggest that air quality degradation is more severe during periods characterized by lower air temperature and slower winds. In contrast, lower overall FRP in northwestern India and weather patterns that result in a higher boundary layer during the pre-monsoon burning season mitigate the transport of pollutants into Delhi. Moreover, for Bengaluru (February to March) and Pune (March to April), FRP within the daily airshed is roughly 46–64% agricultural, but not a selected as a predictor by best subset regression in any of the models. Within the airsheds of these two cities, strong winds and ventilation from the Indian Ocean may help alleviate air quality degradation from outdoor fires. Statistically significant differences in FRP within the daily airshed between extreme and normal pollution days in Delhi during the post-monsoon burning season and lack thereof in all three cities during the pre-monsoon burning season support our conclusions from models constructed from best subset regression and BIC.

We note several limitations of this study: 1) spatiotemporal uncertainties in FRP and susceptibility of FRP to cloud cover and haze, 2) lack of data availability of ground-based air quality measurements, and 3) the applicability of HYSPLIT back trajectory modeling due to potentially high smoke injection heights and mixing of smoke from different source regions. First, we follow the recommendation of Freeborn et al. (2014) to aggregate FRP within the airshed spatially and temporally; temporally, we considered FRP from 4 consecutive days matching daily divisions in the 72-h HYSPLIT back trajectories, and spatially, we extracted the total FRP from a 10-km wide buffer of HYSPLIT back trajectories. However, FRP may be underestimated due to the possible susceptibility of active fire detections to interference from thick haze and cloud cover and active fires below the MODIS detection limit and/or outside satellite overpass times. Second, we address the lack of consistent daily station PM_{10} measurements by calculating a citywide station PM_{10} anomaly. Due to the unreliability of CPCB PM_{10}, we looked at additional air quality-related variables: visibility (NCDC GSOD), AOD (MODIS and AERONET), and $PM_{2.5}$ (US Consulate). We find moderately strong correlation between mean PM_{10} anomalies and $PM_{2.5}$ anomalies in Delhi in 2013 ($r = 0.62$). We also see that correlations of and models using PM_{10} anomalies generally agree with those using visibility and satellite and AERONET AOD. We also

account for the temporal aspect of these two limitations by focusing on the block means for longer averaging windows (3-day, 5-day, and 7-day). Finally, for the third limitation regarding the applicability of HYSPLIT back trajectory analysis, we point to the growing body of literature incorporating HYSPLIT trajectory modeling to analyze the influence of fires. We also find considerable agreement across years in the seasonal airsheds determined from the HYSPLIT back trajectories trace air parcels back to within a season (as defined by > 10% of trajectories), particularly for the pre-monsoon and post-monsoon burning seasons in Delhi's airshed, lending some confidence to our approach.

Our “first-look” approach offers a preliminary analysis of the primary source regions of a city's air pollution that serves to motivate additional in-depth analyses using full atmospheric chemical transport models to attribute health impacts to specific air pollution sources. In this study, we target combustion from regional outdoor fires and more specifically, regional agricultural fires that contribute the majority of FRP to the city airsheds during pre-monsoon and post-monsoon. In contrast to the highly episodic, seasonal nature of agricultural burning, we expect the contribution of some combustion sources, such as waste burning, to be relatively constant throughout the year, while others likely vary seasonally, such as combustion for heating in the winter (December to January). While we focus on a single pollution source on a sub-seasonal timeframe, consideration of other pollution sources throughout the year will be crucial to building emissions inventories and evaluating public health implications in Delhi and other mega-cities.

Combining the approximation of city airsheds using back trajectory modeling with satellite fire observations is a paradigm for assessing the impact of a given pollution source for a given location on a fine spatial scale. In contrast to 3-D dynamic chemical transport models, HYSPLIT is an accessible and computationally inexpensive tool for assessing the regional sources of urban air pollution in India. Future studies could use forward trajectories started from fire hotspots to track transport and estimate the affected region. In addition, for more in-depth analyses, the HYSPLIT batch generator can be used to implement an ensemble-based approach that rapidly incorporates a large number of trajectories that sample temporal and spatial horizontal and vertical variations. This methodology would allow for accessible and near real-time assessment of pollution sources in city airsheds (or airsheds for any specified latitude and longitude) to guide more immediate responses to reduce fires, enforce burning restrictions at the locations and times that are most beneficial to mitigate airshed degradation, and improve local air quality in cities downwind of fires on time scales of days to weeks.

Acknowledgements

This work was supported by the President's Global Innovation Fund at Columbia University and NASA grant NNX11AH98G. The data on winter cropping was supported by NASA grant NNX11AH98G. T. Liu and K. R. Xia were supported by Earth Institute Research Assistantships. The authors gratefully acknowledge the NOAA Air Resources Laboratory (ARL) for the provision of the HYSPLIT transport and dispersion model. We thank P.I. Dr. Panuganti C. S. Devara for establishing and maintaining the Pune AERONET site, the Indian Central Pollution Control Board for access to station PM_{10} data, the U.S. Embassy and Consulates in India for access to station $PM_{2.5}$ data, and the National Climatic Data Center for providing visibility observations. MERRA data used in this study were provided by the Global Modeling and Assimilation Office (GMAO) at NASA Goddard Space Flight Center through the NASA GES DISC online archive. We also thank Natural Earth (naturalearthdata.com) for providing vector files for administrative national and sub-national borders, ocean basins, and coastal borders and Weather Underground (wunderground.com) for historical meteorological data. Finally, we are grateful to Dr. Virendra Sethi, Swetha Pendyala, and Rujuta Chaudhari at IIT-Bombay and Jacob Abaraoha and Dr. Amir Jina for helpful discussions and comments regarding this work.

Appendix A. Supplementary data

Supplementary data related to this article can be found at http://dx.doi.org/10.1016/j.atmosenv.2017.10.024.

References

Atwood, S.A., Reid, J.S., Kreidenweis, S.M., Yu, L.E., Salinas, S.V., Chew, B.N., Balasubramanian, R., 2013. Analysis of source regions for smoke events in Singapore for the 2009 El Niño burning season. Atmos. Environ. 78, 219–230. http://dx.doi.org/10.1016/j.atmosenv.2013.04.047.

Badarinath, K.V.S., Kharol, S.K., Sharma, A.R., 2009. Long-range transport of aerosols from agriculture crop residue burning in Indo-Gangetic Plains—a study using LIDAR, ground measurements and satellite data. J. Atmos. Sol.-Ter. Phys. 71, 112–120. http://dx.doi.org/10.1016/j.jastp.2008.09.035.

Beegum, S.N., Moorthy, K.K., Babu, S.S., Satheesh, S.K., Vinojb, V., Badarinath, K.V.S., Safai, P.D., Devara, P.C.S., Singh, S., Vinod, Dumka, U.C., Pant, P., 2009. Spatial distribution of aerosol black carbon over India during pre-monsoon season. Atmos. Environ. 43, 1071–1078. http://dx.doi.org/10.1016/j.atmosenv.2008.11.042.

Bisht, D.S., Tiwari, S., Dumka, U.C., Srivastava, A.K., Safai, P.D., Ghude, S.D., Chate, D.M., Rao, P.S.P., Ali, K., Prabhakaran, T., Panickar, A.S., Soni, V.K., Attri, S.D., Tunved, P., Chakrabarty, R.K., Hopke, P.K., 2016. Tethered balloon-born and ground-based measurements of black carbon and particulate profiles within the lower troposphere during the foggy period in Delhi, India. Sci. Total Environ. 573, 894–905. http://dx.doi.org/10.1016/j.scitotenv.2016.08.185.

Cady-Pereira, K.E., Payne, V.H., Neu, J.L., Bowman, K.W., Miyazak, K., Marais, E.A., Kulawik, S., Tzompa-Sosa, Z.A., Hegarty, J.D., 2017. Seasonal and spatial changes in trace gases over megacities from Aura TES observations: two case studies. Atmos. Chem. Phys. Discuss. 17, 9379–9398. https://doi.org/10.5194/acp-17-9379-2017.

CIESIN, 2016. Documentation for the Gridded Population of the World, Version 4 (GPWv4). Socioeconomic Data and Applications Centre (SEDAC). Columbia University, Palisades, NY.

CPCB, 2009. National Ambient Air Quality Standards. Online. http://www.cpcb.nic.in/National_Ambient_Air_Quality_Standards.php.

CPCB, 2011. Air Quality Monitoring, Emission Inventory and Source Apportionment Study for Indian Cities. Online. http://cpcb.nic.in/FinalNationalSummary.pdf.

CPCB, 2012. National Ambient Air Quality Status & Trends in India—2010 (National Ambient Air Quality Monitoring NAAQMS/35/2011-2012). Online. http://cpcb.nic.in.

Dey, S., Di Girolamo, L., van Donkelaar, A., Tripathi, S.N., Gupta, T., Mohan, M., 2012. Variability of outdoor fine particulate ($PM_{2.5}$) concentration in the Indian Subcontinent: a remote sensing approach. Remote Sens. Environ. 127, 153–161. http://dx.doi.org/10.1016/j.rse.2012.08.021.

Dotse, S.-Q., Dagar, L., Petra, M.I., De Silvaa, L.C., 2016. Influence of southeast Asian haze episodes on high PM_{10} concentrations across Brunei Darussalam. Environ. Pollut. 219, 337–352. http://dx.doi.org/10.1016/j.envpol.2016.10.059.

Foster, A., Kumar, N., 2011. Health effects of air quality regulations in Delhi, India. Atmos. Environ. 45, 1675–1683. http://dx.doi.org/10.1016/j.atmosenv.2011.01.005.

Freeborn, P.H., Wooster, M.J., Roy, D.P., Cane, M.A., 2014. Quantification of MODIS fire radiative power (FRP) measurement uncertainty for use in satellite-based active fire characterization and biomass burning estimation. Geophys. Res. Lett. 41, 1988–1994. http://dx.doi.org/10.1002/2013GL059086.

Gadde, B., Bonnet, S., Menke, C., Garivait, S., 2009. Air pollutant emissions from rice straw open field burning in India, Thailand and the Philippines. Environ. Pollut. 157, 1554–1558. http://dx.doi.org/10.1016/j.envpol.2009.01.004.

Gargava, P., Rajagopalan, V., 2015a. Source apportionment studies in six Indian cities—drawing broad inferences for urban PM_{10} reductions. Air Qual. Atmos. Health 9, 471–481. http://dx.doi.org/10.1007/s11869-015-0353-4.

Gargava, P., Rajagopalan, V., 2015b. Source prioritization for urban particulate emission control in India based on an inventory of PM_{10} and its carbonaceous fraction in six cities. Environ. Dev. 16, 44–53.

Ghude, S.D., Chate, D.M., Jena, C., Beig, G., Kumar, R., Barth, M.C., Pfister, G.G., Fadnavis, S., Rao, P., 2016. Premature mortality in India due to $PM_{2.5}$ and ozone exposure. Geophys. Res. Lett. 43, 4650–4658. http://dx.doi.org/10.1016/j.envdev.2015.07.009.

Giglio, L., 2007. Characterization of the tropical diurnal fire cycle using VIRS and MODIS observations. Remote Sens. Environ. 108, 407–421. http://dx.doi.org/10.1016/j.rse.2006.11.018.

Gurjar, B.R., Ravindra, K., Nagpure, A.S., 2016. Air pollution trends over Indian mega-cities and their local-to-global implications. Atmos. Environ. 142, 475–495. http://dx.doi.org/10.1016/j.atmosenv.2016.06.030.

Guttikunda, S.K., Jawahar, P., 2012. Application of SIM-air modeling tools to assess air quality in Indian cities. Atmos. Environ. 62, 551–561. http://dx.doi.org/10.1016/j.atmosenv.2012.08.074.

Guttikunda, S.K., Jawahar, P., 2014. Atmospheric emissions and pollution from the coal-fired thermal power plants in India. Atmos. Environ. 92, 449–460. http://dx.doi.org/10.1016/j.atmosenv.2014.04.057.

Guttikunda, S.K., Goel, R., Pant, P., 2014. Nature of air pollution, emission sources, and management in the Indian cities. Atmos. Environ. 95, 501–510. http://dx.doi.org/10.

1016/j.atmosenv.2014.07.006.
Hansen, M.C., Potapov, P.V., Moore, R., Hancher, M., Turubanova, S.A., Tyukavina, A., Thau, D., Stehman, S.V., Goetz, S.J., Loveland, T.R., Kommareddy, A., Egorov, A., Chini, L., Justice, C.O., Townshend, J.R.G., 2013. High-resolution global maps of 21st-century forest cover change. Science 342, 850–853. http://dx.doi.org/10.1126/science.1244693.
Hays, M., Fine, P., Geron, C., Kleeman, M., Gullett, B., 2005. Open burning of agricultural biomass: physical and chemical properties of particle-phase emissions. Atmos. Environ. 39, 6747–6764. http://dx.doi.org/10.1016/j.atmosenv.2005.07.072.
Holben, B., Eck, T., Slutsker, I., Tanre, D., Buis, J., Setzer, A., Vermote, E., Reagan, J., Kaufman, Y., Nakajima, T., 1998. AERONET—a federated instrument network and data archive for aerosol characterization. Remote Sens. Environ. 66, 1–16. http://dx.doi.org/10.1016/S0034-4257(98)00031-5.
Jain, M., Mondal, P., DeFries, R.S., Small, C., Galford, G.L., 2013. Mapping cropping intensity of smallholder farms: a comparison of methods using multiple sensors. Remote Sens. Environ. 134, 210–223. http://dx.doi.org/10.1016/j.rse.2013.02.029.
Jain, M., Mondal, P., Galford, G.L., Fiske, G., DeFries, R.S., 2017. An automated approach to map winter cropped area of smallholder farms across large scales using MODIS imagery. Remote Sens. 9, 566. https://doi.org/10.3390/rs9060566.
Kaskaoutis, D.G., Kumar, S., Sharma, D., Singh, R.P., Kharol, S.K., Sharma, M., Singh, A.K., Singh, S., Singh, A., Singh, D., 2014. Effects of crop residue burning on aerosol properties, plume characteristics, and long-range transport over northern India. J. Geophys. Res. Atmos. 119, 5424–5444. http://dx.doi.org/10.1002/2013JD021357.
Kishcha, P., Silva, A.M., Starobinets, B., Alpert, P., 2014. Air pollution over the Ganges basin and northwest Bay of Bengal in the early postmonsoon season based on NASA MERRAero data. J. Geophys. Res. Atmos. 119, 1555–1570. http://dx.doi.org/10.1002/2013JD020328.
Kumar, R., Barth, M.C., Pfister, G.G., Nair, V.S., Ghude, S.D., Ojha, N., 2015a. What controls the seasonal cycle of black carbon aerosols in India? J. Geophys. Res. Atmos. 120, 7788–7812. http://dx.doi.org/10.1002/2015JD023298.
Kumar, P., Kumar, S., Joshi, L., 2015b. Socioeconomic and Environmental Implications of Agricultural Residue Burning: a Case Study of Punjab, India.
Kusumaningtyas, S.D.A., Aldrian, E., 2016. Impact of the June 2013 Riau province Sumatera smoke haze event on regional air pollution. Environ. Res. Lett. 11, 1–11. http://dx.doi.org/10.1088/1748-9326/11/7/075007.
Kutner, M.H., Nachtsheim, C.J., Neter, J., 2004. Applied Linear Regression Models, fourth ed. McGraw-Hill Irwin.
Lelieveld, J., Evans, J.S., Fnais, M., Giannadaki, D., Pozzer, A., 2015. The contribution of outdoor air pollution sources to premature mortality on a global scale. Nature 525, 367–371. http://dx.doi.org/10.1038/nature15371.
Levy, R.C., Mattoo, S., Munchak, L.A., Remer, L.A., Sayer, A.M., Patadia, F., Hsu, N.C., 2013. The Collection 6 MODIS aerosol products over land and ocean. Atmos. Meas. Tech. 6, 2989–3034. http://dx.doi.org/10.5194/amt-6-2989-2013.
Lu, Z., Streets, D.G., 2012. Increase in NO_x emissions from Indian thermal power plants during 1996–2010: unit-based inventories and multisatellite observations. Environ. Sci. Technol. 46, 7463–7470. http://dx.doi.org/10.1021/es300831w.
Menard, S., 2002. Applied Logistic Regression Analysis. SAGE Publications Inc.
Miller, A.J., 1984. Subset selection in regression. J. R. Stat. Soc. A 147, 389–425. http://dx.doi.org/10.2307/2981576.
Miller, D.J., Sun, K., Zondlo, M.A., Kanter, D., Dubovik, O., Welton, E.J., Winker, D.M., Ginoux, P., 2011. Assessing boreal forest fire smoke aerosol impacts on U.S. air quality: a case study using multiple data sets. J. Geophys. Res. Atmos. 116, D22209,. http://dx.doi.org/10.1029/2011JD016170.
Mishra, A.K., Shibata, T., 2012. Synergistic analyses of optical and microphysical properties of agricultural crop residue burning aerosols over the Indo-Gangetic Basin (IGB). Atmos. Environ. 57, 205–218. http://dx.doi.org/10.1016/j.atmosenv.2012.04.025.
Mishra, V., Smoliak, B., Lettenmaier, D., Wallace, J., 2012. A prominent pattern of year-to-year variability in Indian Summer monsoon rainfall. Proc. Natl. Acad. Sci. U. S. A. 109, 7213–7217. http://dx.doi.org/10.1073/pnas.1119150109.
Mittal, S.K., Singh, N., Agarwal, R., Awasthi, A., Gupta, P.K., 2009. Ambient air quality during wheat and rice crop stubble burning episodes in Patiala. Atmos. Environ. 238–244. http://dx.doi.org/10.1016/j.atmosenv.2008.09.068.
Mondal, P., Jain, M., DeFries, R.S., Galford, G.L., Small, C., 2015. Sensitivity of crop cover to climate variability: insights from two Indian agro-ecoregions. J. Env. Manage. 148, 21–30. http://dx.doi.org/10.1016/j.jenvman.2014.02.026.
Pan, X.L., Kanaya, Y., Wang, Z.F., Komazaki, Y., Taketani, F., Akimoto, H., Pochanart, P., 2013. Variations of carbonaceous aerosols from open crop residue burning with transport and its implication to estimate their lifetimes. Atmos. Environ. 74, 301–310. http://dx.doi.org/10.1016/j.atmosenv.2013.03.048.
Rienecker, M.M., Suarez, M.J., Gelaro, R., Todling, R., Bacmeister, J., Liu, E., Bosilovich, M.G., Schubert, S.D., Takacs, L., Kim, G., Bloom, S., Chen, J., Collins, D., Conaty, A., da Silva, A., Gu, W., Joiner, J., Koster, R.D., Lucchesi, R., Molod, A., Owens, T., Pawson, S., Pegion, P., Redder, C.R., Reichle, R., Robertson, F.R., Ruddick, A.G., Sienkiewicz, M., Woollen, J., 2011. MERRA—NASA's modern-era retrospective analysis for Research and applications. J. Clim. 24, 3624–3648. http://dx.doi.org/10.1175/JCLI-D-11-00015.1.
Rolph, G.D., 2016. Real-time Environmental Applications and Display SYstem (READY). Online. NOAA Air Resources Laboratory, College Park, MD. http://www.ready.noaa.gov.
Safai, P.D., Kewat, S., Praveen, P.S., Rao, P.S.P., Momin, G.A., Ali, K., Devara, P.C.S., 2007. Seasonal variation of black carbon aerosols over a tropical urban city of Pune, India. Atmos. Environ. 41, 2699–2709. http://dx.doi.org/10.1016/j.atmosenv.2006.11.044.
Sahani, M., Zainon, N.A., Mahiyuddin, W.R.W., Latif, M.T., Hod, R., Khan, M.F., Tahir, N.M., Chan, C.-C., 2014. A case-crossover analysis of forest fire haze events and mortality in Malaysia. Atmos. Environ. 96, 257–265. http://dx.doi.org/10.1016/j.atmosenv.2014.07.043.
Sapkota, A., Morel Symons, J., Kleissl, J., Wang, L., Parlange, M.B., Ondov, J., Breysse, P.N., Diette, G.B., Eggleston, P.A., Buckley, T.J., 2005. Impact of the 2002 Canadian forest fires on particulate matter air quality in Baltimore city. Environ. Sci. Technol. 39, 24–32. http://dx.doi.org/10.1021/es035311z.
Schneider, A., Friedl, M.A., Potere, D., 2010. Monitoring urban areas globally using MODIS 500m data: new methods and datasets based on urban ecoregions. Remote Sens. Environ. 114, 1733–1746. http://dx.doi.org/10.1016/j.rse.2010.03.003.
Schwarz, G., 1978. Estimating the dimension of a model. Ann. Stat. 6, 461–464. Retrieved from. http://www.jstor.org/stable/2958889.
Sharma, M., Dikshit, O., 2016. Comprehensive Study on Air Pollution and Green House Gases (GHGs) in Delhi. Online. http://delhi.gov.in/DoIT/Environment/PDFs/Final_Report.pdf.
Singh, R.P., Kaskaoutis, D.G., 2014. Crop residue burning: a threat to South Asian air quality. EOS 95, 333–340.
Stein, A.F., Draxler, R.R., Rolph, G.D., Stunder, B.J.B., Cohen, M.D., Ngan, F., 2015. NOAA's HYSPLIT atmospheric transport and dispersion modelling system. Bull. Amer. Meteor. Soc. 96, 2059–2077. http://dx.doi.org/10.1175/BAMS-D-14-00110.1.
Tiwari, S., Bisht, D.S., Srivastava, A.K., Shivashankara, G.P., Kumar, R., 2013. Interannual and intraseasonal variability in fine mode particles over Delhi: influence of meteorology. Adv. Meteor. 2013, 1–9. http://dx.doi.org/10.1155/2013/740453.
Tiwari, S., Bisht, D.S., Srivastava, A.K., Gustafsson, Ö., 2014a. Simultaneous measurements of black carbon and $PM_{2.5}$, CO, and NO_x variability at a locally polluted urban location in India. Nat. Hazards 75, 813–829. http://dx.doi.org/10.1007/s11069-014-1351-9.
Tiwari, S., Bisht, D.S., Srivastava, A.K., Shivashankara, G.P., Pipal, A.S., Taneja, A., Srivastava, M.K., Attri, S.D., 2014b. Variability in atmospheric particulates and meteorological effects on their mass concentrations over Delhi, India. Atmos. Res. 145–146, 45–46. http://dx.doi.org/10.1016/j.atmosres.2014.03.027.
United Nations, Department of Economic and Social Affairs, Population Division, 2015. World Population Prospects: the 2015 Revision. Key Findings and Advance Tables Working Paper No. ESA/P/WP.241. .
Vadrevu, K.P., Badarinath, K.V.S., Anuradha, E., 2008. Spatial patterns in vegetation fires in the Indian region. Environ. Monit. Assess. 147, 1–13. http://dx.doi.org/10.1007/s10661-007-0092-6.
Vadrevu, K.P., Csiszar, I., Ellicott, E., Giglio, L., Badarinath, K.V.S., Vermote, E., Justice, C., 2013. Hotspot analysis of vegetation fires and intensity in the Indian region IEEE. J. Sel. Top. Appl. Earth Obs. Remote Sens. 6, 224–238. http://dx.doi.org/10.1109/JSTARS.2012.2210699.
Vadrevu, K.P., Ellicott, E., Badarinath, K., 2011. MODIS derived fire characteristics and aerosol optical depth variations during the agricultural residue burning season, North India. Environ. Pollut. 159, 1560–1569. http://dx.doi.org/10.1016/j.envpol.2011.03.001.
Venkataraman, C., Habib, G., Kadamba, D., Shrivastava, M., Leon, J.F., Crouzille, B., Boucher, O., Streets, D.G., 2006. Emissions from open biomass burning in India: integrating the inventory approach with high-resolution Moderate Resolution Imaging Spectroradiometer (MODIS) active-fire and land cover data. Glob. Biogeochem. Cy. 20, GB2013. http://dx.doi.org/10.1029/2005GB002547.
Vijayakumar, K., Safai, P.D., Devara, P.C.S., Rao, S.V.B., Jayasankar, C.K., 2016. Effects of agriculture crop residue burning on aerosol properties and long-range transport over northern India: a study using satellite data and model simulations. Atmos. Res. 178–179, 155–163. http://dx.doi.org/10.1016/j.atmosres.2016.04.003.
Wentz, F.J., Scott, J., Hoffman, R., Leidner, M., Atlas, R., Ardizzone, J., 2015. Remote Sensing Systems Cross-calibrated Multi-platform (CCMP) 6-hourly Ocean Vector Wind Analysis Product on 0.25 Deg Grid, Version 2.0., Remote Sensing Systems. Santa Rosa, CA. Online. www.remss.com/measurements/ccmp, Accessed date: 2 October 2016.
WMO, 1996. Guide to Meteorological Instruments and Methods of Observation, sixth ed. 92-63-16008-2 loose-leaf.
Wooster, M.J., Roberts, G., Perry, G.L.W., Kaufman, Y.J., 2005. Retrieval of biomass combustion rates and totals from fire radiative power observations: FRP derivation and calibration relationships between biomass consumption and fire radiative energy release. J. Geophys. Res. 110, D24311. http://dx.doi.org/10.1029/2005JD006318.
World Health Organization, 2006. Air Quality Guidelines for Particulate Matter, Ozone, Nitrogen Dioxide and Sulphur Dioxide.
World Health Organization, 2016. Ambient Air Pollution: a Global Assessment of Exposure and Burden of Disease.